THE JOURNAL OF BIOLOGICAL CHEMISTRY VOL. 282, NO. 2, pp. 1119–1127, January 12, 2007

Mutant Presenilin 1 Alters Synaptic Transmission in Cultured Hippocampal Neurons*

Received for publication, May 26, 2006, and in revised form, October 31, 2006 Published, JBC Papers in Press, November 6, 2006, DOI 10.1074/jbc.M605066200

Christina Priller[‡], Ilse Dewachter[§], Neville Vassallo[¶], Sandra Paluch[‡], Claudia Pace[‡], Hans A. Kretzschmar[‡], Fred Van Leuven[§], and Jochen Herms[‡1]

From the [‡]Department of Neuropathology, Ludwig-Maximilians-Universität Munich, Feodor-Lynen-Strasse 23, 81377 München, Germany, the [§]Experimental Genetics Group, KULeuven-Campus Gasthuisberg, B-3000 Leuven, Belgium, and the [¶]Department of Physiology and Biochemistry, University of Malta, Msida MSD06, Malta

Mutations in presenilins are the major cause of familial Alzheimer disease, but the precise pathogenic mechanism by which presenilin (PS) mutations cause synaptic dysfunction leading to memory loss and neurodegeneration remains unclear. Using autaptic hippocampal cultures from transgenic mice expressing human PS1 with the A246E mutation, we demonstrate that mutant PS1 significantly depressed the amplitude of evoked α-amino-3-hydroxy-5-methyl-4-isoxazolepropionic acid and *N*-methyl-D-aspartate receptor-mediated synaptic currents. Analysis of the spontaneous miniature synaptic activity revealed a lower frequency of miniature currents but normal miniature amplitude. Both alterations could be rescued by the application of a γ-secretase blocker. On the other hand, the application of synthetic soluble $A\beta_{42}$ in wild-type neurons induced the PS1 mutant phenotype on synaptic strength. Together, these findings strongly suggest that the expression of mutant PS1 in cultured neurons depresses synaptic transmission by causing a physical reduction in the number of synapses. This hypothesis is consistent with morphometic and semiquantitative immunohistochemical analysis, revealing a decrease in synaptophysin-positive puncta in PS1 mutant hippocampal neurons.

Alzheimer disease is an age-related neurodegenerative disorder characterized clinically by a progressive deterioration in memory and other cognitive abilities. Neuropathological hallmarks include a progressive loss of neurons, synaptic degeneration, and deposition of amyloid plaques and neurofibrillary tangles in characteristic brain regions. Dominantly inherited mutations in presenilin (PS)[2] 1 and 2 are the primary cause of familial Alzheimer disease (1). The exact pathogenic mechanism by which PS mutations cause memory loss and neurodegeneration, however, remains unclear.

Presenilins are integral components of a multiprotein protease complex termed γ-secretase that is responsible for the intramembranous cleavage of the amyloid precursor protein (APP) and the Notch receptors (2, 3). Familial Alzheimer disease-linked PS mutations selectively enhance the production of the amyloidogenic 42-residue β-amyloid peptide ($A\beta_{42}$), often at the expense of the less amyloidogenic $A\beta_{40}$ generation (4, 5), suggesting a toxic gain-of-function pathogenic mechanism. In mammalian cells mutant forms of PS1 produce reduced levels of the intracellular domains of Notch and APP, which can function as transcriptional activators (4–6).

Neuropathological studies have indicated that synaptic abnormalities may represent the proximate cause of dementia in Alzheimer disease. Synaptic loss correlates better with the pattern and severity of cognitive impairment than formation of amyloid plaques or neurofibrillary tangles (7). In addition, synaptic and dendritic loss precedes neuronal loss and is most prominent in limbic regions corresponding to the clinical deficits (7, 8).

Abnormalities in learning and synaptic function have been observed in transgenic mice expressing mutant APP or mutant PS1. However, the results obtained by different groups using different animal models are very heterogeneous. For instance, initial studies examining long-term potentiation, a widely used model for synaptic plasticity, reported a reduction of long-term potentiation in transgenic mice with Aβ accumulation (9–11), indicating that an alteration in synaptic plasticity may underlie memory deficits in transgenic Alzheimer disease mice. However, later studies were not able to reproduce these findings fully; rather, they pointed to an impairment of basal synaptic transmission in these mice (12–18). In transgenic mice expressing mutant PS1 alone, long-term potentiation was even found to be facilitated (19–21). The heterogeneity of the findings in different experimental settings may be due to the possibility that mutant PS1 exerts pathogenic effects not only by increasing $A\beta_{42}$ production but also by influencing synapse formation or synaptic plasticity (22, 23).

Here we aimed to analyze pre- and postsynaptic mechanisms of synaptic vesicle release in mutant PS1 transgenic mice in detail by studying autapses in single-grown hippocampal neurons. Autapses are synapses between the axon and dendrites of the same neuron. These structures are built when neurons are cultured separately, a condition that is achieved by a special coating of the cell culture wells. The main advantage compared with conventional preparations is that these monosynaptic cultures ensure that the release from the same set of synapses is

* This work was supported by Deutsche Forschungsgemeinschaft Grant SFB 596 and the Bayerische Forschungsverbunt ForPrion. The costs of publication of this article were defrayed in part by the payment of page charges. This article must therefore be hereby marked "*advertisement*" in accordance with 18 U.S.C. Section 1734 solely to indicate this fact.

[1] To whom correspondence should be addressed. Tel.: 89-2180-78010; Fax: 89-2180-78037; E-mail: jochen.herms@med.uni-muenchen.de.

[2] The abbreviations used are: PS, presenilin; APP, amyloid precursor protein; DIV, days *in vitro*; RRP, releasable vesicle pool; DAPT, [*N*-(3,5-difluorophenacetyl-L-alanyl)]-*S*-phenylglycine *t*-butyl ester; NMDA, *N*-methyl-D-aspartate; AMPA, α-amino-3-hydroxy-5-methyl-4-isoxazolepropionic acid; EPSC, excitatory post-synaptic current; mEPSC, miniature EPSC; non-tg, non-transgenic; PS1wt, wild-type human PS1; PS1mut, mutant human PS1.

monitored regardless of the stimulation method and in absence of complex polysynaptic circuitry. Our results essentially show that mutant PS1 strongly affects both the amplitude of evoked excitatory currents as well as the frequency of spontaneous excitatory synaptic currents by decreasing the number of functional synapses.

EXPERIMENTAL PROCEDURES

Mice—The parent PS1 transgenic mice (wild-type human PS1 and human mutant PS1[A246E]) were generated by microinjection of mini-gene constructs containing PS1 cDNA in a mouse Thy1 gene cassette into prenuclear embryos as described (10, 24). Transgenic strains were maintained on the FVB/N background and back-crossed to obtain homozygous mice for either wild-type (PS1wt) or mutant human PS1 (PS1mut). FVB/N mice were used as non-transgenic (Non-tg) controls.

Cell Culture—Microisland cultures of mouse hippocampal neurons were prepared and maintained as described (25, 26). Briefly, astrocyte feeder wells enriched in type 1 astrocytes (>95%) were first prepared from postnatal day 1 mouse hippocampal tissue. After dissection and removal of the choroid plexus and meninges, the material was dissociated and trypsinized. Astrocytes were grown in culture media consisting of Dulbecco's modified Eagle's medium with 4.5 g/liter glucose (Pan, Aidenbach, Germany), 5% fetal bovine serum (Pan), 100 IU/ml penicillin/streptomycin (Invitrogen), N2 supplement (Invitrogen), Glutamax (Invitrogen), and Mito$^+$ serum extender (BD Bioscience) at their indicated concentrations. Astrocytes were grown at 37 °C in a 10% CO_2-enriched atmosphere. Once a monolayer was achieved in the flasks, cells were trypsinized and replated onto microdot-coated glass coverslips. Hippocampi were dissected from newborn mice pups and digested in Dulbecco's modified Eagle's medium solution containing 0.2 mg/ml cysteine, 100 mM $CaCl_2$, 50 mM EDTA, 10units/ml papain (Roche Applied Science) at 37 °C. Digestion was stopped after 60 min, and tissue was gently triturated using fire-polished Pasteur pipettes. Cell suspensions diluted to $5–8 \times 10^4$ cells/ml were then added to the prepared astrocyte feeder wells (see above). To prevent excessive proliferation of astrocytes, the anti-mitotic agent 5-fluoro-2′-deoxyuridine (8.1 mM) was applied to the cultures on the day after neuronal plating. For the γ-secretase inhibitor experiment, autaptic cultures were incubated with 1 μM *N*-[*N*-(3,5-difluorophenacetyl-L-alanyl)]-*S*-phenylglycine *t*-butyl Ester (DAPT, Calbiochem) 48 h before the measurements. For the Aβ incubation studies, freshly diluted monomeric $A\beta_{42}$ (100 nM, Bachem, Switzerland) was added to the autaptic cultures ,and electrophysiological measurements were carried out after 48 h.

Electrophysiology—For each experiment approximately equal numbers of cells from the respective genotypes were measured in parallel and blindly on the same day *in vitro* (18–20 days *in vitro* (DIV). Whole-cell recordings were performed using an EPC 9 amplifier (HEKA Elektronic, Lambrecht, Germany). The standard extracellular medium contained 140 mM NaCl, 2.4 mM KCl, 10 mM HEPES, 10 mM glucose, 4 mM $CaCl_2$, 4 mM $MgCl_2$, and 15 μM bicuculline, 300 mosM, pH 7.3. NMDA-excitatory post-synaptic currents (EPSCs) were measured at 4 mM external Ca^{2+} in the presence of 5 μM 6-cyano-7-nitroquinoxaline-2,3-dione, 10 μM glycine and in the absence of external Mg^{2+}. Internal pipette recording solution consisted of 10 mM NaCl, 125 mM potassium gluconate, 1 mM EGTA, 4.6 mM $MgCl_2$, 4 mM Na_2ATP, 15 mM creatine phosphate, and 20 mM units/ml phosphocreatine kinase, 300 mosM, pH 7.3. Data were filtered at 2 kHz and acquired at 10 kHz using Pulse 8.5 software (HEKA Elektronic). Patch electrodes had resistances of 3–4 megohms. Series resistance and capacity of the electrodes were compensated; only recordings with access resistance below 15 megohms and with an initial membrane potential <-50 mV (measured in the current-clamp modus shortly after cell access was obtained) were included in the analysis. Access resistance and cell capacities (5–25 picofarads) were compensated. Cells were voltage-clamped at −70 mV, except for 1-ms depolarizations to 0 mV to elicit an action potential-like stimulus. The rise time constant (10–90%) of the synaptic currents was determined by fitting a linear function to the activating current, and the decay time constant was determined by fitting a single exponential function to the current decay. Detection of miniature EPSCs was usually performed for at least 60 s in the presence of 200 nM tetrodotoxin (Biotrend, Köln, Germany). Data were analyzed with a template detection program (Axograph 4.1, Axon Instruments, Sunnyvale, CA). Threshold for detection was set to 3.5 times the base-line S.D. Captured miniature EPSCs (mEPSCs) of individual cells were averaged to determine mean amplitude and charge per cell. Application of a hypertonic solution for pool size determination was made by pulsed application of 500 mM sucrose to the extracellular solution for 4 s using a fast perfusion system (Warner Instruments, Hamden, CT). Evoked responses and responses to hypertonic sucrose solutions were always recorded successively from the same cell. The readily releasable vesicle pool (RRP) per cell was calculated by dividing the charge of the transient sucrose response with the mean mEPSC charge of the same cell, if available. To further determine the mean vesicular release probability, the number of vesicles released by a single action potential-like stimulus was divided by the number of vesicles in the RRP. Recordings and data analysis were performed blindly on each sample.

Immunocytochemistry—Hippocampal cultures of 18–20 DIV were used for immunocytochemistry. For fluorescent microscopic determinations of synaptic density in neurons, cultures were fixed for 10 min with 4% paraformaldehyde, blocked, and permeabilized with phosphate-buffered saline containing 2% bovine serum albumin, 10% goat serum (Dako Hamburg, Germany), 0.3% Triton X-100 (Calbiochem) for 30 min. Cells were incubated with rabbit polyclonal anti microtubule-associated protein 2 (1:100, Chemicon, Hampshire, UK) for 60 min, washed with phosphate-buffered saline, and incubated with fluorescein isothiocyanate-conjugated goat anti-rabbit IgG (1:100) for another 60 min. After another washing step, fluorescent-labeled mouse monoclonal anti-synaptophysin (1:1000, Synaptic Systems, Göttingen, Germany) was added, incubated for 60 min, and finally fixed in fluorescent mounting medium (Dako). Images were acquired on an Axiovert 200M microscope (Zeiss, Oberkochen, Germany) with a 63× LD Achroplan objective and Axiovision 4.5 software (Zeiss). For quantification of the total dendritic length and total amount of

synapses, analySIS software (Soft Imaging System, Münster, Germany) was used. The summary graph represents four independent experiments using different culture preparations from PS1mut animals and PS1wt controls. All chemicals were obtained from Sigma-Aldrich unless otherwise noted.

Immunohistochemistry—Six hemispheres (3 of each genotype) of 30-day- and 3-month-old wild-type human PS1, human mutant PS1[A246E], and controls were removed and fixed in 4% paraformaldehyde overnight. Coronal 50-μm free floating sections were prepared with a VT 1000S vibratome (Leica, Wetzlar, Germany) and immunostained with anti-synaptophysin and Cy^{TM}3-conjugated streptavidin. Briefly, sections were placed in phosphate-buffered saline, blocked with antibody diluent (Ventana Medical Systems, Inc., Illkirch, France), and then incubated overnight at 4 °C with the polyclonal antibody against synaptophysin (1:300, Chemicon). This step was followed by incubation in biotinylated swine anti-rabbit IgG (1:150, Dako), and finally, the sections were fluorescence labeled with Cy^{TM}3-conjugated streptavidin (1:25, Dianova, Hamburg, Germany). The sections were mounted on precoated glass slides (Super-frost-plus, Menzel, Braunschweig, Germany) and covered (Coverquick, Labonord, Templemars, France). All sections were processed simultaneously under the same conditions. The immunofluorescent labeling protocol was repeated three times to assess the reproducibility of results. Immunolabeled brain sections were viewed with a Zeiss 40×/0.8 IR Achroplan objective on a Zeiss Axioskop 2FS mot LSM510 confocal microscope.

Cy3 was excited with a HeNe Laser at 543 nm, and the emitted fluorescence was detected with a LP560 (longpass 560 nm) emission filter. Frames of 230 × 230-μm size were scanned with 0.22 μm/pixel, and the pinhole diameter was set to an area unit of 1. The *z*-distance of each *z*-stack ranged from 10 to 15 μm and consisted of 20–30 0.5-μm-spaced images.

Synaptophysin levels were assessed as described previously (27)in the stratum radiatum and stratum moleculare of the hippocampus in three coronal sections per animal. Two serial optical *z*-stacks (one for each marker) of the synaptophysin-labeled structures were collected from each section. All series of *z*-stacks from each section were maximum intensity projected and acquired under standard conditions maintaining the same gain, aperture, and black level settings. This method of analysis was previously evaluated by Masliah *et al.* (28, 29). The digitized images were then analyzed regarding the signal intensity and density (covered area of immunohistochemistry-positive objects) of synaptophysin-labeled structures (PictureAnalyzer Software, Bjarne Krebs, Zentrum für Neuropathologie und Prion Forschung, Munich, Germany). A threshold was set so that all objects with an intensity value below the threshold were set equal to the background value. For each mouse, the values obtained for the stratum radiatum and stratum moleculare of the hippocampus were averaged.

Western Blot—For measurement of the expression of synaptophysin in hippocampus, coronal brain sections were collected on glass slides and Nissl stained. The hippocampal region was then separately lysed and subjected to SDS-PAGE as previously reported (30). After electrotransfer of proteins to the polyvinylidene difluoride membrane, immunoblotting was followed by the incubation with primary antibody against synaptophysin (1:5000, Chemicon) and β-actin (1:5000, actin I-19, Santa Cruz Biotechnology, Heidelberg, Germany) overnight. The visualization was performed with a secondary antibody coupled to alkaline phosphatase (polyclonal goat anti-mouse and anti-rabbit immunoglobulin/alkaline phosphatase, Dako) and chromogene nitro blue tetrazolium salt with 5-bromo-4-chloro-3-indolylphosphate. Western blots were scanned with a high resolution flatbed scanner, and the density of bands was determined using Total Lab Version 2.01 software (Nonlinear Dynamics, Newcastle-upon-Tyne, UK).

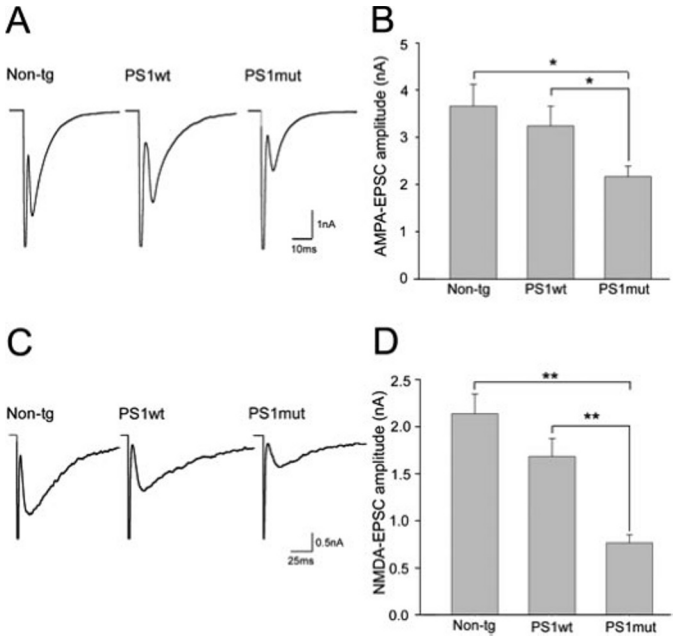

FIGURE 1. **Evoked neurotransmitter release in Non-tg neurons and in neurons expressing PS1wt or PS1mut.** *A*, representative AMPA-EPSC traces from Non-tg, PS1wt, and PS1mut neurons. *B*, AMPA-EPSC amplitude in neurons from Non-tg (n = 19), PS1wt (n = 30), and PS1mut (n = 41) mice. *C*, representative NMDA-EPSC traces from Non-tg, PS1wt, and PS1mut neurons. *D*, NMDA-EPSC amplitude in neurons from Non-tg (n = 15), PS1wt (n = 32), and PS1mut (n = 27) mice (*, $p < 0.05$; **, $p < 0.005$).

Statistical Analysis—All error bars indicate the S.E. All results are reported as ± S.E. A value <0.05 was considered as statistically significant (Student's *t* test).

RESULTS

Evoked Neurotransmitter Release in Non-tg, PS1wt, and PS1mut Neurons—Patch clamp recordings from single isolated neurons were used to assess possible defects in neurotransmitter release induced by mutant PS1. We concentrated our analysis on glutamatergic neurons, because they are much more abundant in autaptic cultures than in inhibitory cells producing γ-aminobutyric acid. We first tested the action potential-evoked neurotransmitter release. AMPA and NMDA synaptic responses were evoked by brief somatic depolarization (1-ms depolarization from −70mV holding potential to 0 mV) and measured as peak inward currents a few ms after action potential induction (Fig. 1, *A* and *C*). The amplitude of the evoked autaptic amplitudes of AMPA-EPSCs was reduced in PS1mut cells compared with neurons expressing human PS1wt and Non-tg mice (3.66 ± 0.46 nA for Non-tg, 3.24 ± 0.42 nA for PS1wt, and

2.16 ± 0.22 nA for PS1mut; $p < 0.05$; Fig. 1*B*). Similarly, NMDA receptor-mediated EPSCs, analyzed by blocking AMPA receptors by 6-cyano-7-nitroquinoxaline-2,3-dione (5 μM), revealed a significantly reduced amplitude in PS1 mutant cells when compared with cells from mice expressing human wild-type PS1 or from non-transgenic mice (2.14 ± 0.28 nA for Non-tg, 1.68 ± 0.19 nA for PS1wt, and 0.77 ± 0.08 nA for PS1mut; $p < 0.05$; Fig. 1*D*). No significant differences were observed in the kinetics (rise time and decay time constant τ) of both AMPA and NMDA receptor-mediated EPSCs between PS1 mutant, PS1 wild-type, and non-transgenic neurons (Table 1).

Thus, the strength of excitatory synaptic transmission was found to be decreased in autaptic hippocampal neurons expressing mutant hPS1. Factors possibly influencing this change include (i) a decrease in postsynaptic responsiveness, (ii) an alteration in presynaptic release parameters, and (iii) a lower number of synapses.

Spontaneous Neurotransmitter Release in Non-tg, PS1wt, and PS1mut Neurons—To define whether the pre- or the postsynaptic side is affected by mutant PS1, we analyzed the amplitude and frequency of spontaneous mEPSC activity (*mEPSCs*; Fig. 2*A*). We found that the frequency of mEPSCs was significantly lower in PS1mut neurons than in hPS1 and non-transgenic cells (8.03 ± 1.52 s^{-1} for Non-tg, 7.95 ± 1.53 s^{-1} for PS1wt, and 3.02 ± 0.59 s^{-1} for PS1mut neurons; $p < 0.05$; Fig. 2*B*). The mean mEPSC amplitude, however, was not affected (24.34 ± 0.87 pA for Non-tg, 23.36 ± 0.92 pA for PS1wt, and 25.06 ± 1.12 pA for PS1mut cells; $p > 0.05$; Fig. 2*C*), indicating that the responsiveness and number of postsynaptic receptors is not altered due to mutation of PS1. In addition, we calculated the number of vesicles released by an action potential-like stimulus by dividing the charge of evoked responses by that of a single mEPSC. For those neurons in which both EPSCs and mEPSCs were measured, the quantity of vesicles released during an EPSC was determined and found to be significantly lower in PS1mut neurons (526 ± 148 for Non-tg, 481 ± 111 for PS1wt, and 169 ± 68 for PS1mut cells; $p < 0.05$; Fig. 2*D*).

TABLE 1
Summary of evoked EPSC kinetics
Data are expressed as the mean ± S.E., n = 15–27 cells/genotype.

	Rise time	τ
	ms	*ms*
AMPA EPSC		
Non-tg	2.06 ± 0.19	7.25 ± 0.97
PS1wt	2.14 ± 0.24	8.20 ± 0.67
PS1mut	2.15 ± 0.21	6.72 ± 0.44
NMDA EPSC		
Non-tg	7.66 ± 0.95	61.19 ± 3.55
PS1wt	8.03 ± 1.09	63.95 ± 4.89
PS1mut	7.01 ± 0.92	60.88 ± 4.39

Readily Releasable Vesicle Pool and Release Probability in Non-tg, PS1wt, and PS1mut Neurons—Presynaptic release is thought to depend on the size of the RRP and the release probability (P_r). We, therefore, performed a detailed analysis of the sizes of RRPs in neurons of Non-tg, PS1wt, and PS1mut neurons. The fact that the mEPSC rates were significantly different between the three genotypes suggested that the size of the RRP pool is changed in the presence of PS1mut. The sizes of RRP were quantified by measuring the response of Non-tg, hPS1, and PS1mut cells to pulsed application of 500 mM hypertonic sucrose solution for 3–4 s. This treatment induces the release of the entire pool of readily releasable vesicles, which in turn leads to a transient inward current followed by a steady current component (31, 32) (Fig. 3*A*). We calculated the amount of RRP vesicles by dividing the total charge of the transient current component after application of hypertonic sucrose by the charge of a single mEPSC measured from the same cell. Neurons from PS1mut mice showed significantly less releasable vesicles in their RRP compared with neurons from non-transgenic and PS1 wild-type mice (24.72 ± 5.61 × 10^3 for Non-tg, 16.15 ± 3.18 × 10^3 for PS1wt, and 8.14 ± 2.11 × 10^3 for PS1mut; $p < 0.05$; Fig. 3*B*). No differences were observed in the basal rate of RRP refilling, which was estimated by averaging the ratio of the charge of a second hypertonic sucrose response over the initial sucrose response measured 3.5 s prior (0.57 ± 0.05 for Non-tg, 0.55 ± 0.02 for PS1wt, and 0.57 ± 0.04 for PS1mut; $p > 0.05$; Fig. 3*C*).

To estimate whether the efficiency of the action potential-induced vesicle release is influenced by PS1 mutation, we analyzed the vesicular release probability (P_{vr}).

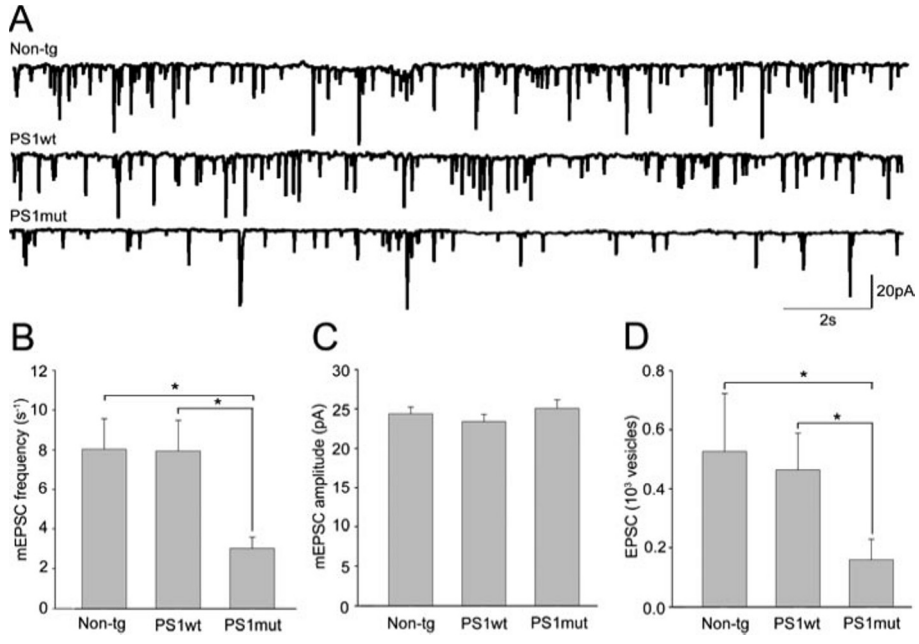

FIGURE 2. **Spontaneous neurotransmitter release in Non-tg neurons and in neurons expressing PS1wt or PS1mut.** *A*, representative mEPSC traces from Non-tg, PS1wt, and PS1mut neurons. *B*, mEPSC frequency in neurons from Non-tg (n = 22), PS1wt (n = 24), and PS1mut (n = 30) mice. *C*, mEPSC amplitude in neurons from Non-tg (n = 22), PS1wt (n = 24), and PS1mut mice (n = 30) mice. *D*, estimated EPSC vesicles for Non-tg (n = 9), PS1wt (n = 11), and PS1mut mice (n = 8)(*, $p < 0.05$).

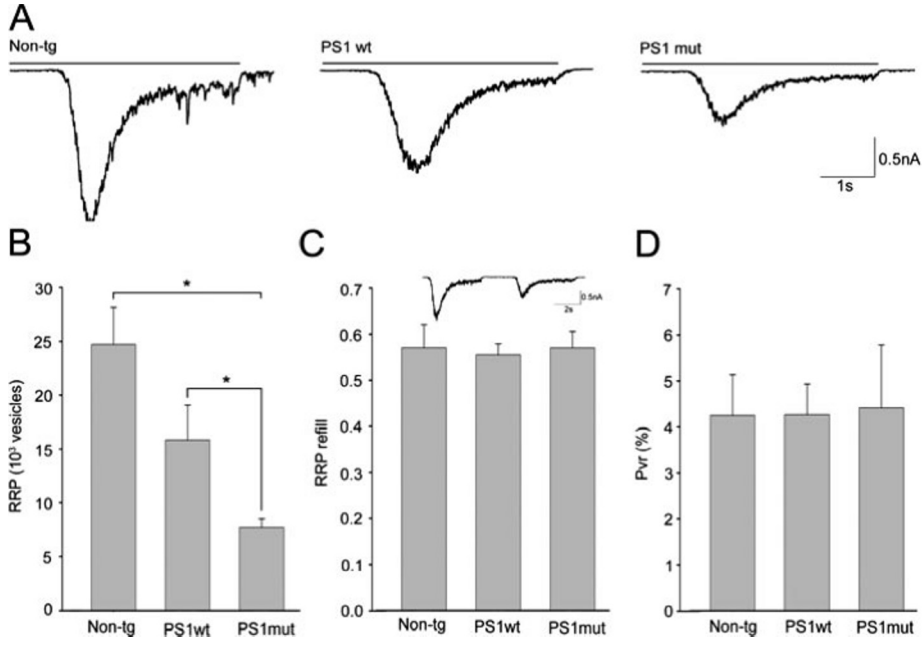

FIGURE 3. **Estimated RRP, RRP refilling, and release probability in Non-tg neurons and in neurons expressing PS1wt or PS1mut.** *A*, representative raw traces of responses to hypertonic solution from Non-tg, PS1wt, and PS1mut neurons. Hypertonic solution was applied for 4 s as indicated by the *black bar*. *B*, estimated RRP vesicles for Non-tg ($n = 26$), PS1wt ($n = 18$), and PS1mut ($n = 29$) mice. *C*, average ratio of the second hypertonic sucrose response to the initial sucrose response measured 4 s before (the *inset* shows sample recording). *D*, *bar diagram* showing the average vesicular release probability (P_{vr}) of Non-tg ($n = 9$), PS1wt ($n = 11$), and PS1mut ($n = 8$) mice (*, $p < 0.05$).

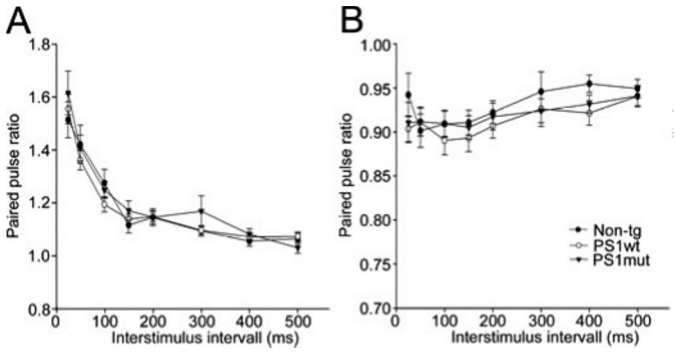

FIGURE 4. **Paired pulse ratio of Non-tg neurons and neurons expressing PS1wt or PS1mut.** *A*, average EPSC amplitudes of Non-tg ($n = 18$), PS1wt ($n = 24$), and PS1mut ($n = 40$) neurons to different stimulus intervals at 1 mM $[Ca^{2+}]_e$ normalized to the size of the first response. *B*, average EPSC amplitudes of Non-tg ($n = 12$), PS1wt ($n = 16$), and PS1mut ($n = 18$) neurons to different stimulus intervals at 4 mM $[Ca^{2+}]_e$ normalized to the size of the first response.

We determined P_{vr} by dividing the number of vesicles released during an action potential by the number of vesicles in the RRP. We found that P_{vr} did not vary significantly between cells from non-transgenic (4.24 ± 0.89%), PS1wt (4.25% ± 0.67%), and PS1mut neurons (4.41 ± 1.37%; Fig. 3*D*). The P_{vr} values obtained are similar to the values obtained in other studies on autaptic hippocampal neurons (33). In summary, these results indicate that the content of presynaptic vesicles seems to be released efficiently and that the decrease in synaptic responses in PS1mut autapses can be attributed to the decrease in RRP.

Paired Pulse Stimulation in Non-tg, PS1wt, and PS1mut Neurons—Changes in the synaptic release probability of a neuron may cause concomitant changes in short-term plasticity of synaptic transmission. Trains of action potentials lead to facilitation in synapses with low initial release probability but to depression in synapses with high initial release probability. By applying paired pulses with 25- 500-ms intervals to the cultured neurons, the paired-pulse ratio, defined as relative amplitude of the second EPSC normalized to the first EPSC, was obtained and compared between non-transgenic, PS1wt, and PS1mut neurons. No significant differences in the paired-pulse ratio were observed between neurons from Non-tg, PS1wt, and PS1mut mice both at low extracellular Ca^{2+} concentration, leading to paired pulse facilitation (Fig. 4*A*), and at high extracellular Ca^{2+} concentration, leading to paired pulse depression (Fig. 4*B*).

Prolonged Repetitive and High Frequency Stimulation in Non-tg, PS1wt, and PS1mut Neurons—Repetitive stimulation gives insights into the nature of the release probability, P_r, and the size of the RRP in the central synapse (34). For prolonged repetitive stimulation we used a 10-Hz protocol, and for high frequency stimulation we used a 50-Hz protocol at 4 mM $[Ca^{2+}]_{out}$ (Fig. 5, *A* and *C*). There was no significant difference in the gradual reduction of the relative EPSC amplitude during repetitive stimulation at 10 Hz between Non-tg, PS1wt, and in PS1mut neurons (Fig. 5*B*). Similar properties were observed in evoked responses elicited by high frequency stimulation at 50 Hz (Fig. 5*D*).

γ-Secretase Inhibitor Enhances Evoked and Spontaneous Neurotransmitter Release in PS1mut Neurons—To determine whether the reduction of EPSC amplitude is caused by γ-secretase cleavage products, we blocked γ-secretase activity in PS1mut neurons by the addition of 1 μM DAPT. DAPT-treated PS1mut neurons showed significantly higher AMPA-EPSC responses compared with untreated PS1mut neurons (1.83 ± 0.26 nA for control PS1mut and 2.65 ± 0.28 nA for DAPT-treated PS1mut; $p < 0.05$; Fig. 6*A*). The frequency of spontaneous neurotransmitter release was also found to be increased in DAPT-treated PS1mut neurons (1.72 ± 0.49 s^{-1} for control PS1mut and 4.28 ± 0.98 s^{-1} for DAPT-treated PS1mut neurons; $p < 0.05$; Fig. 6*B*). Both results indicate that the PS1mutant phenotype can be rescued by inhibiting γ-secretase activity.

The addition of $A\beta_{42}$ Decreases Evoked and Spontaneous Neurotransmitter Release in PS1mut Neurons—If the DAPT effect of rescuing the PS1mut phenotype is mediated by a decreased production and extracellular release of Aβ peptides, then monomeric $A\beta_{42}$ should negatively affect synaptic function in non-transgenic cells. Indeed, non-transgenic neurons treated with $A\beta_{42}$ (100 nM) showed a significant

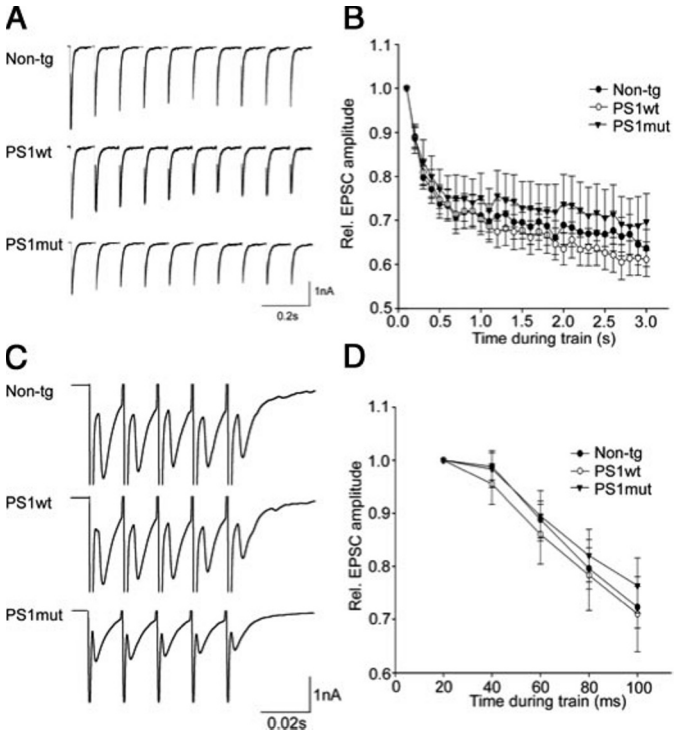

FIGURE 5. **Prolonged repetitive and high frequency stimulation of Non-tg neurons and neurons expressing PS1wt or PS1mut.** *A*, sample recordings of the first 10 responses in a 10 Hz train. *B*, average EPSC amplitudes of Non-tg ($n = 16$), PS1wt ($n = 25$), and PS1mut ($n = 32$) during 10-Hz train normalized to the size of first response. *C*, sample recordings of 5 responses in a 50-Hz train. *D*, average EPSC amplitudes of Non-tg ($n = 21$), PS1wt ($n = 28$), and PS1mut ($n = 35$) during 50-Hz train normalized to the size of first response.

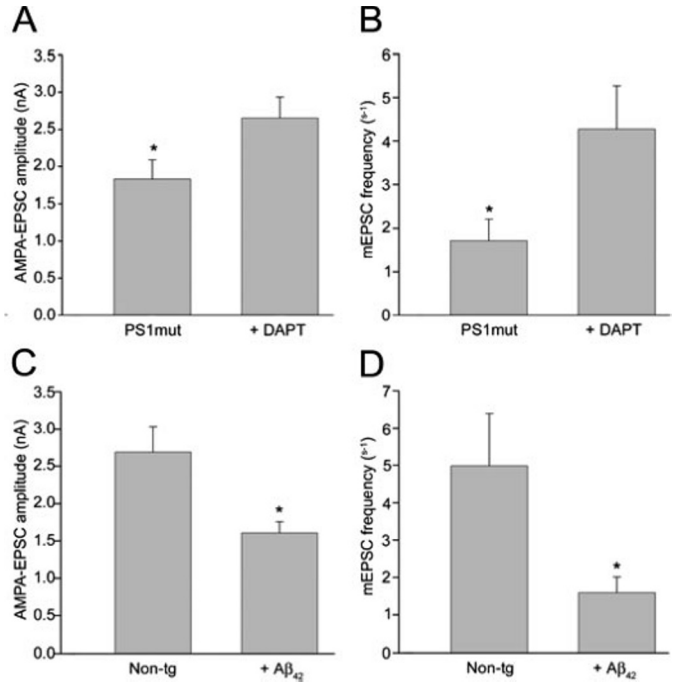

FIGURE 6. **Evoked and spontaneous neurotransmitter release in neurons treated either with DAPT or Aβ_{42}.** *A*, AMPA-EPSC amplitude in neurons from control PS1mut ($n = 27$) and PS1mut neurons treated with DAPT ($n = 25$). *B*, mEPSC frequency in control PS1mut neurons ($n = 22$) and PS1mut neurons treated with DAPT ($n = 22$). *C*, AMPA-EPSC amplitude in control Non-tg neurons ($n = 9$) and Non-tg neurons treated with Aβ_{42} ($n = 11$). *D*, mEPSC frequency in control Non-tg neurons ($n = 9$) and Non-tg neurons treated with Aβ_{42} ($n = 10$) (*, $p < 0.05$).

reduction in AMPA-EPSC responses compared with untreated non-transgenic neurons (2.69 ± 0.34 nA for control Non-tg and 1.61 ± 0.15 nA for Aβ-treated Non-tg neurons; $p < 0.05$; Fig. 6*C*). The frequency of spontaneous neurotransmitter release was also significantly lower in non-transgenic neurons treated with Aβ_{42} (4.98 ± 1.4 s^{-1} for control Non-tg and 1.60 ± 0.41 s^{-1} for Aβ-treated Non-tg cells; $p < 0.05$; Fig. 6*D*). In summary, Aβ_{42} applied extracellularly reduces both the amplitude and the frequency of excitatory synaptic currents in autaptic hippocampal cultures of non-transgenic mice, thus mimicking the effect of mutant PS1.

Reduced Number of Synapses per Dendritic Length in PS1mut Neurons—Based on the evidence of a decrease in evoked EPSCs and smaller RRP in PS1mut autapses, we quantified synaptic densities using immunohistochemical markers. Cultures were double-stained with antibodies to the presynaptic marker synaptophysin and the dendritic marker microtubule-associated protein 2 (Fig. 7*A*), and the number of synapses per 10 μm was counted. PS1wt neurons showed significantly more synaptophysin-positive puncta per 10 μm than PS1mut cells (1.20 ± 0.07 for PS1wt and 0.98 ± 0.05 for PS1mut; $p < 0.05$; Fig. 7*B*).

Staining Intensity and Expression of Synaptophysin in the Hippocampus of PS1mut Mice—To demonstrate that the decrease in synapse formation in cultured PS1mut neurons is also present *in vivo*, we performed immunohistochemistry on floating sections of 1-month and 3-month-old wild-type, PS1mut, and PS1wt animals. We then analyzed synaptophysin levels in the stratum radiatum and the stratum moleculare of the hippocampus by confocal microscopy (Fig. 8). The average staining intensity of synaptophysin-positive presynaptic termini in the stratum radiatum was found to be reduced by 34% in 1-month-old PS1mut mice compared with PS1wt mice (61.06 ± 4.49% for PS1mut and 96.84 ± 1.95% for PS1wt; $p < 0.005$; Fig. 8*B*). In 3-month-old animals the expression of synaptophysin was still significantly reduced in the stratum radiatum but only by 9% (83.39 ± 5.76% for PS1mut and 92.52 ± 1.57% for PS1wt; $p < 0.05$; Fig. 8*B*). Evaluation of the average synaptophysin-staining intensity in the stratum moleculare revealed no significant differences both in 1- and in 3-month-old PS1mut and PS1wt mice (Fig. 8*C*). To corroborate the histological difference of synaptophysin expression in PS1mut mice compared with PS1wt mice, we performed Western blots from the hippocampal region. The relative expression of synaptophysin in comparison to β-actin was determined by densitometric measurements in four independently prepared Western blots from three 1-and 3-month-old PS1mut and PS1wt mice. As shown in Fig. 8*D*, we observed significantly lower levels of synaptophysin in PS1mut samples both at 1 and at 3 months of age compared with PS1wt samples (0.87 ± 0.02 for PS1wt and 0.72 ± 0.04 for PS1mut in 1 month-old animals and 0.89 ± 0.06 for PS1wt and 0.67 ± 0.08 for PS1mut in 1 month-old animals, $p < 0.05$). Altogether, these results are consistent with a reduced synapse formation of PS1mut hippocampal neurons.

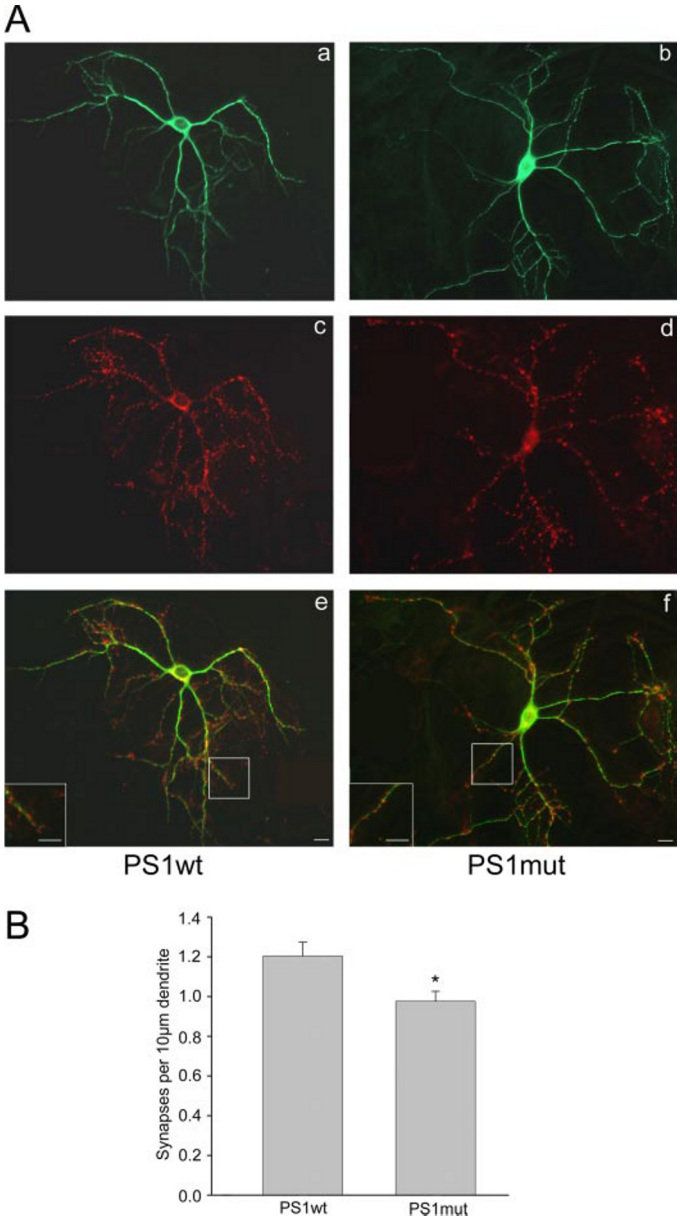

FIGURE 7. **Structural analysis of synapses in microisland cultures from PS1wt and PS1mut neurons.** *A*, immunostains of autaptic neurons. *Aa* and *Ab*, staining for the dendritic marker microtubule-associated protein 2 to assess the size of PS1wt and PS1mut neurons. *Ac* and *Ad*, staining of the same culture for synaptophysin to assess the number of synapses. *Ae* and *Af*, merged picture of microtubule-associated protein 2 and synaptophysin staining. *Scale bar*, 25 μm. *B*, density of synapses on dendrites measured as number of synaptophysin-positive spots per 10 μm dendrite from PS1wt (n = 56) and PS1mut (n = 63) neurons from three independent preparations (*, $p < 0.05$).

DISCUSSION

Our study has primarily shown that excitatory synaptic transmission in cultured hippocampal neurons expressing mutant PS1 is markedly inhibited. Both the amplitude of evoked excitatory synaptic currents as well as the frequency of spontaneous synaptic currents were decreased. In line with these findings, we observed a significant reduction in pool size of synaptic vesicles per neuron, whereas the synaptic and vesicular release probability (and, hence, efficiency) remained unchanged. Altogether these results primarily indicate that mutant PS1 does not affect presynaptic mechanisms of synaptic transmission. Moreover, we have no indication of involvement of a postsynaptic mechanism, either for instance, a reduced number or function of glutamate receptors, since the mini EPSC amplitude was not found to be altered by expression of mutant PS1. We also did 3-(4,5-dimethylthiazol-2-yl)-2,5-diphenyltetrazolium bromide viability assays on cultured neurons expressing wild-type or mutant PS1 and found no differences in survival (data not shown). Therefore, a general impairment in cell health of the transfected neurons is unlikely. Finally, quantitative immunohistochemical analysis of cultured autaptic neurons and of brain slices from 1- and 3-month-old mice support the notion that the above electrophysiological observations are most likely due to a physical decrease in the number of functional synapses. However, why does mutant PS1 only affect synapse density more strongly in young animals than in older ones? In young animals, mutant PS1 most likely results in a reduced formation of synapses during the early stages of brain formation. In the developing brain, however, a physiological mechanism operates that eliminates those synapses that are inactive (35). This mechanism would reduce the number of synapses that have been formed in surplus during early brain development according to neuronal activity. Such a reduction would be expected to be less in mutant PS1 mice because fewer synapses have been formed in early development. Therefore, in older animals the difference in synaptic density between PS1mut and PS1wt mice would be decreased. This may also be the explanation why our electrophysiological data contrasts with previous observations performed on slice preparations of adult mutant PS1 mouse brains, which revealed no significant alterations in basal synaptic transmission in adult transgenic mice expressing mutant PS1 (19, 36).

The ensuing question is: how can mutant PS1 affect the formation of excitatory synapses in cultured neurons? A recent electrophysiological study on cultured neurons of PS1 knockout mice favors a gain-of-function hypothesis for explaining our results (37). The enhanced mEPSC frequency as well as enhanced synapse formation observed (37) corroborate our observation that the mutant PS1 defect in synaptic strength can be rescued by inhibition of γ-secretase activity. Therefore, a pathological gain-of-function has to be considered, pertaining to four possible mechanisms. First, mutant PS1 affects synaptic formation due to enhanced generation of Aβ_{42} at the expense of Aβ_{40} (38). Second, altered generation of other APP cleavage products, for example reduced generation of the C-terminal cleavage product AICD (APP intracellular domain), may be critical (4). Third, mechanisms secondary to alterations in the intracellular calcium storage, as described in cells expressing mutant PS1, may be involved (21, 39–42). Fourth, cleavage of other substrates of the γ-secretase complex could be involved, *e.g.* Notch1 and homologs, Notch ligands Jagged2 and Delta, ErbB4, CD44, low density lipoprotein receptor-related protein, N- and E-cadherins, nectin-1α, p75 neurotrophin receptor, syndecan3, telencephalin, and deleted in colorectal cancer (DCC) (43). A loss-of-function mechanism in PS1-mediated cleavage of any of these proteins cannot account for the reduced synaptic responses in mutant PS1 neurons, since we

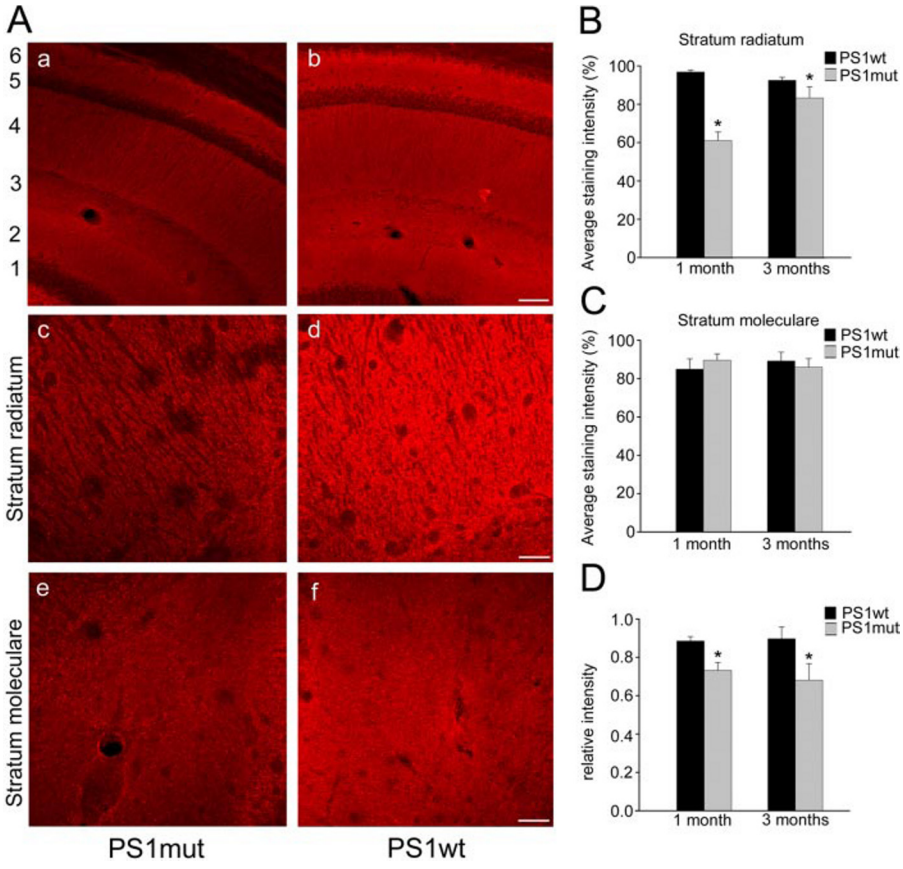

FIGURE 8. **Synaptophysin staining of sections derived from PS1wt and PS1mut mice.** *A*, synaptophysin-positive presynaptic terminals in mouse hippocampus. *Aa* and *Ab*, low magnification view of PS1wt and PS1mut hippocampus from 1-month-old mice: *1*, stratum granulosum; *2*, stratum moleculare; *3*, stratum lacunosum; *4*, stratum radiatum; *5*, stratum pyramidale; *6*, stratum oriens. *Scale bar*, 100 μm. *Ac* and *Ad*, synaptophysin staining of the stratum radiatum from 1-month-old PS1wt and PS1mut mice. *Ac* and *Ad*, synaptophysin-positive presynaptic terminals in the stratum radiatum and stratum moleculare (*Ae* and *Af*) of 1-month-old PS1wt and PS1mut mice. *Scale bar*, 25 μm. *B*, average staining intensity in the stratum radiatum of PS1wt (n = 18 areas, 9 sections) and PS1mut (n = 18 areas; 9 sections) mice at the age of 1 and 3 months, respectively. *C*, average staining intensity in the stratum moleculare of PS1wt (n = 18 areas, 9 sections) and PS1mut (n = 18 areas, 9 sections) mice at the age of 1 and 3 months, respectively. *D*, Western blot analysis of synaptophysin expression relative to β-actin in hippocampal brain sections of three PS1wt and PS1mut mice of 1 and 3 months of age. Relative band intensity of synaptophysin expression normalized to β-actin levels revealed a lower expression of synaptophysin in PS1mut mice compared with PS1wt both at 1 and in 3 months of age mice (*, $p < 0.05$).

show that the reduced synaptic response in mutant PS1 can be rescued by the application of γ-secretase blocker. The involvement of alterations in calcium storage by mutant PS1 (21, 41, 42), however, cannot be excluded.

Based on our results that application of synthetic soluble Aβ_{42} induced the same effect as the expression of mutant PS1, we favor the hypothesis that enhanced Aβ_{42} generation of mutant PS1 neurons must be critical. This is supported by recent experimental approaches of other groups either applying soluble Aβ directly, analyzing transgenic mice with high Aβ_{42} production, or by analyzing APP-transfected neurons. After application of soluble Aβ_{42} to cultured cortical neurons, an acute reduction in NMDA receptor currents in cultured cortical neurons were observed (44). On the other hand, in hippocampal CA1 neurons from adult APP(K670N/M671L) × PS1(P264) double transgenic mice, a depression of AMPA receptor-mediated synaptic currents was observed without alterations in NMDA receptor-mediated synaptic currents (45). Depression of both AMPA and NMDA receptor-mediated synaptic currents was observed in organotypic hippocampal slices expressing APP by infection with Sindbis viral vector (46). All these studies proposed that the function of excitatory synapses is modulated by soluble Aβ. In contrast, electrophysiological study on autaptic hippocampal neurons by us as well as on transfected slice preparations (46) indicated that the function of glutaminergic postsynaptic receptors was not altered. Rather, we propose that Aβ_{42} modulates the number of synapses either by affecting the formation of new synapses or by provoking the degeneration of existing ones. A reduction in synapse number may involve a transient and gradual decrease in postsynaptic receptor expression or function. Indeed, synapse formation and remodeling is known to depend at least on the activation of excitatory amino acid receptors (35). It has been recently shown that soluble Aβ alters the molecular composition of glutaminergic synapses within 1 h (47, 48). Thus, this phenomenon could indeed hold true for the reduction of the number of synapses we observe in cultured neurons challenged with Aβ_{42} for several days.

This study analyzing synaptic transmission in mutant PS1 transgenic mice further supports the idea that soluble Aβ_{40} may play a normal physiological role in synapse formation and maintenance. This role can become compromised by decreased production of Aβ_{40} and/or by increased generation of Aβ_{42}, particularly oligomer formation, thus altering Aβ function from a beneficial to a pathological one (49). This toxic gain-of-function of Aβ in synapse formation and remodeling underscores the need for therapeutic attempts aimed at reducing the level of Aβ_{42} in this cellular compartment, thereby preventing synaptic degeneration and ameliorating cognitive deficits in Alzheimer disease. In light of the accumulating evidence for a physiological role of Aβ_{40} in modulating synaptic strength (44–48), methods for preferentially decreasing Aβ_{42} without affecting Aβ_{40} production are needed. This may include the generation of specific antibodies targeted against oligomeric Aβ_{42} or the use of selective γ-secretase inhibitors.

Acknowledgments—We thank Dr. Michael Mansour for helpful suggestions throughout the project, Dr. Gerda Mitteregger for excellent support in animal breeding, and the late Doris Schechinger for excellent technical assistance.

REFERENCES

1. Hardy, J., and Gwinn-Hardy, K. (1998) *Science* **282,** 1075–1079
2. De Strooper, B., Saftig, P., Craessaerts, K., Vanderstichele, H., Guhde, G., Annaert, W., von Figura, K., and Van Leuven, F. (1998) *Nature* **391,** 387–390
3. De Strooper, B., Annaert, W., Cupers, P., Saftig, P., Craessaerts, K., Mumm, J. S., Schroeter, E. H., Schrijvers, V., Wolfe, M. S., Ray, W. J., Goate, A., and Kopan, R. (1999) *Nature* **398,** 518–522
4. Moehlmann, T., Winkler, E., Xia, X., Edbauer, D., Murrell, J., Capell, A., Kaether, C., Zheng, H., Ghetti, B., Haass, C., and Steiner, H. (2002) *Proc. Natl. Acad. Sci. U. S. A.* **99,** 8025–8030
5. Schroeter, E. H., Ilagan, M. X., Brunkan, A. L., Hecimovic, S., Li, Y. M., Xu, M., Lewis, H. D., Saxena, M. T., De Strooper, B., Coonrod, A., Tomita, T., Iwatsubo, T., Moore, C. L., Goate, A., Wolfe, M. S., Shearman, M., and Kopan, R. (2003) *Proc. Natl. Acad. Sci. U. S. A.* **100,** 13075–13080
6. Cao, X., and Sudhof, T. C. (2001) *Science* **293,** 115–120
7. Terry, R. D., Masliah, E., Salmon, D. P., Butters, N., DeTeresa, R., Hill, R., Hansen, L. A., and Katzman, R. (1991) *Ann. Neurol.* **30,** 572–580
8. Braak, E., and Braak, H. (1997) *Acta Neuropathol.* (*Berl.*) **93,** 323–325
9. Chapman, P. F., White, G. L., Jones, M. W., Cooper-Blacketer, D., Marshall, V. J., Irizarry, M., Younkin, L., Good, M. A., Bliss, T. V., Hyman, B. T., Younkin, S. G., and Hsiao, K. K. (1999) *Nat. Neurosci.* **2,** 271–276
10. Moechars, D., Dewachter, I., Lorent, K., Reverse, D., Baekelandt, V., Naidu, A., Tesseur, I., Spittaels, K., Haute, C. V., Checler, F., Godaux, E., Cordell, B., and Van Leuven, F. (1999) *J. Biol. Chem.* **274,** 6483–6492
11. Nalbantoglu, J., Tirado-Santiago, G., Lahsaini, A., Poirier, J., Goncalves, O., Verge, G., Momoli, F., Welner, S. A., Massicotte, G., Julien, J. P., and Shapiro, M. L. (1997) *Nature* **387,** 500–505
12. Fitzjohn, S. M., Morton, R. A., Kuenzi, F., Rosahl, T. W., Shearman, M., Lewis, H., Smith, D., Reynolds, D. S., Davies, C. H., Collingridge, G. L., and Seabrook, G. R. (2001) *J. Neurosci.* **21,** 4691–4698
13. Hsia, A. Y., Masliah, E., McConlogue, L., Yu, G. Q., Tatsuno, G., Hu, K., Kholodenko, D., Malenka, R. C., Nicoll, R. A., and Mucke, L. (1999) *Proc. Natl. Acad. Sci. U. S. A.* **96,** 3228–3233
14. Larson, J., Lynch, G., Games, D., and Seubert, P. (1999) *Brain Res.* **840,** 23–35
15. Roder, S., Danober, L., Pozza, M. F., Lingenhoehl, K., Wiederhold, K. H., and Olpe, H. R. (2003) *Neuroscience* **120,** 705–720
16. Gong, B., Vitolo, O. V., Trinchese, F., Liu, S., Shelanski, M., and Arancio, O. (2004) *J. Clin. Investig.* **114,** 1624–1634
17. Trinchese, F., Liu, S., Battaglia, F., Walter, S., Mathews, P. M., and Arancio, O. (2004) *Ann. Neurol.* **55,** 801–814
18. Gureviciene, I., Ikonen, S., Gurevicius, K., Sarkaki, A., van Groen, T., Pussinen, R., Ylinen, A., and Tanila, H. (2004) *Neurobiol. Dis.* **15,** 188–195
19. Parent, A., Linden, D. J., Sisodia, S. S., and Borchelt, D. R. (1999) *Neurobiol. Dis.* **6,** 56–62
20. Barrow, P. A., Empson, R. M., Gladwell, S. J., Anderson, C. M., Killick, R., Yu, X., Jefferys, J. G., and Duff, K. (2000) *Neurobiol. Dis.* **7,** 119–126
21. Schneider, I., Reverse, D., Dewachter, I., Ris, L., Caluwaerts, N., Kuiperi, C., Gilis, M., Geerts, H., Kretzschmar, H., Godaux, E., Moechars, D., Van Leuven, F., and Herms, J. (2001) *J. Biol. Chem.* **276,** 11539–11544
22. Saura, C. A., Choi, S. Y., Beglopoulos, V., Malkani, S., Zhang, D., Shankaranarayana Rao, B. S., Chattarji, S., Kelleher, R. J., III, Kandel, E. R., Duff, K., Kirkwood, A., and Shen, J. (2004) *Neuron* **42,** 23–36
23. Marjaux, E., Hartmann, D., and De Strooper, B. (2004) *Neuron* **42,** 189–192
24. Dewachter, I., Van Dorpe, J., Smeijers, L., Gilis, M., Kuiperi, C., Laenen, I., Caluwaerts, N., Moechars, D., Checler, F., Vanderstichele, H., and Van Leuven, F. (2000) *J. Neurosci.* **20,** 6452–6458
25. Rosenmund, C., Clements, J. D., and Westbrook, G. L. (1993) *Science* **262,** 754–757
26. Rosenmund, C., Feltz, A., and Westbrook, G. L. (1995) *J. Neurophysiol.* **73,** 427–430
27. Priller, C., Bauer, T., Mitteregger, G., Krebs, B., Kretzschmar, H. A., and Herms, J. (2006) *J. Neurosci.* **26,** 7212–7221
28. Masliah, E., Terry, R. D., Mallory, M., Alford, M., and Hansen, L. A. (1990) *Am. J. Pathol.* **137,** 1293–1297
29. Masliah, E., Terry, R. D., Alford, M., and DeTeresa, R. (1990) *J. Histochem. Cytochem.* **38,** 837–844
30. Krebs, B., Kohlmannsperger, V., Nolting, S., Schmalzbauer, R., and Kretzschmar, H. A. (2006) *J. Histochem. Cytochem.* **54,** 559–565
31. Bekkers, J. M., and Stevens, C. F. (1991) *Proc. Natl. Acad. Sci. U. S. A.* **88,** 7834–7838
32. Rosenmund, C., and Stevens, C. F. (1996) *Neuron* **16,** 1197–1207
33. Reim, K., Mansour, M., Varoqueaux, F., McMahon, H. T., Sudhof, T. C., Brose, N., and Rosenmund, C. (2001) *Cell* **104,** 71–81
34. Schneggenburger, R., Meyer, A. C., and Neher, E. (1999) *Neuron* **23,** 399–409
35. Cohen-Cory, S. (2002) *Science* **298,** 770–776
36. Zaman, S. H., Parent, A., Laskey, A., Lee, M. K., Borchelt, D. R., Sisodia, S. S., and Malinow, R. (2000) *Neurobiol. Dis.* **7,** 54–63
37. Parent, A. T., Barnes, N. Y., Taniguchi, Y., Thinakaran, G., and Sisodia, S. S. (2005) *J. Neurosci.* **25,** 1540–1549
38. Murayama, O., Tomita, T., Nihonmatsu, N., Murayama, M., Sun, X., Honda, T., Iwatsubo, T., and Takashima, A. (1999) *Neurosci. Lett.* **265,** 61–63
39. Herms, J., Schneider, I., Dewachter, I., Caluwaerts, N., Kretzschmar, H., and Van Leuven, F. (2003) *J. Biol. Chem.* **278,** 2484–2489
40. Leissring, M. A., Murphy, M. P., Mead, T. R., Akbari, Y., Sugarman, M. C., Jannatipour, M., Anliker, B., Muller, U., Saftig, P., De Strooper, B., Wolfe, M. S., Golde, T. E., and LaFerla, F. M. (2002) *Proc. Natl. Acad. Sci. U. S. A.* **99,** 4697–4702
41. Leissring, M. A., Paul, B. A., Parker, I., Cotman, C. W., and LaFerla, F. M. (1999) *J. Neurochem.* **72,** 1061–1068
42. LaFerla, F. M. (2002) *Nat. Rev. Neurosci.* **3,** 862–872
43. Vetrivel, K. S., Cheng, H., Kim, S. H., Chen, Y., Barnes, N. Y., Parent, A. T., Sisodia, S. S., and Thinakaran, G. (2005) *J. Biol. Chem.* **280,** 25892–25900
44. Snyder, E. M., Nong, Y., Almeida, C. G., Paul, S., Moran, T., Choi, E. Y., Nairn, A. C., Salter, M. W., Lombroso, P. J., Gouras, G. K., and Greengard, P. (2005) *Nat. Neurosci.* **8,** 1051–1058
45. Chang, E. H., Savage, M. J., Flood, D. G., Thomas, J. M., Levy, R. B., Mahadomrongkul, V., Shirao, T., Aoki, C., and Huerta, P. T. (2006) *Proc. Natl. Acad. Sci. U. S. A.* **103,** 3410–3415
46. Kamenetz, F., Tomita, T., Hsieh, H., Seabrook, G., Borchelt, D., Iwatsubo, T., Sisodia, S., and Malinow, R. (2003) *Neuron* **37,** 925–937
47. Almeida, C. G., Tampellini, D., Takahashi, R. H., Greengard, P., Lin, M. T., Snyder, E. M., and Gouras, G. K. (2005) *Neurobiol. Dis.* **20,** 187–198
48. Roselli, F., Tirard, M., Lu, J., Hutzler, P., Lamberti, P., Livrea, P., Morabito, M., and Almeida, O. F. (2005) *J. Neurosci.* **25,** 11061–11070
49. Huang, S. M., Mouri, A., Kokubo, H., Nakajima, R., Suemoto, T., Higuchi, M., Staufenbiel, M., Noda, Y., Yamaguchi, H., Nabeshima, T., Saido, T. C., and Iwata, N. (2006) *J. Biol. Chem.* **281,** 17941–17951